Journal of Applied Data Sciences
Vol. 7, No. 3, September 2026, pp. 1964-1979

GoogLeNetMP: A Development of GoogLeNet Architecture for Multi-Class Microplastic Classification in Subsurface Water Image

Halifia Hendri[1,*], Yuhandri[2], Agung Ramadhanu[3]

[1]*Computer System Department, Universitas Putra Indonesia YPTK, Padang, Indonesia*

[2]*Doctor of Information Technology Department, Universitas Putra Indonesia YPTK, Padang, Indonesia*

[3]*Master of Informatics Enngineering Department, Universitas Putra Indonesia YPTK, Padang, Indonesia*

(Received: March 1, 2026; Revised: April 25, 2026; Accepted: June 25, 2026; Available online: July 12, 2026)

Abstract

Microplastic pollution has become a major environmental concern due to its persistence in marine ecosystems and its potential impact on aquatic organisms and human health. Automatic detection of microplastic particles in underwater environments remains challenging because of turbidity, low contrast, light distortion, and the visual similarity between microplastics and natural marine objects. This study proposes GoogLeNetMP, an enhanced GoogLeNet-based deep learning architecture for multi-class classification of subsurface marine images into four categories: primary microplastics, secondary microplastics, non-microplastics, and marine biota. The proposed framework integrates basic image preprocessing (resizing and noise reduction) with a modified GoogLeNetMP architecture designed to intrinsically handle fine-grained feature extraction under degraded conditions, thereby minimizing the reliance on complex external enhancement pipelines. A dataset of underwater images acquired from the coastal waters of Padang, Indonesia, was used for model development and evaluation. Experimental results show that GoogLeNetMP outperformed the standard GoogLeNet model, achieving 95.75% accuracy, 92.80% sensitivity, 97.00% specificity, and an F1-score of 92.06%. The proposed model also demonstrated more stable training convergence and better discrimination of visually challenging classes. The architecture is designed to internalize the robust feature extraction process, thereby minimizing the reliance on extensive external enhancement pipelines while maintaining standard normalization steps for input consistency. These findings indicate that GoogLeNetMP is a promising approach for AI-based marine pollution monitoring and decision support in sustainable coastal management.

Keywords: Googlenetmp, Microplastic Classification, Underwater Image Analysis, Marine Pollution Monitoring, Convolutional Neural Network, Subsurface Marine Imaging.

1. Introduction

Microplastic contamination of marine ecosystems has rapidly escalated into one of the most critical and highly topical environmental crises worldwide. Microplastics, strictly defined as plastic debris with dimensions of less than 5 millimeters, originate from the direct manufacturing of consumer goods as well as the continuous degradation of larger macroplastics driven by environmental weathering [1]. Recent modeling estimates suggest that the global ocean surface may contain between 82 and 358 trillion plastic particles. However, these figures are subject to significant uncertainty ranges due to differences in sampling methodologies, such as varying net mesh sizes and spatial modeling approaches [2]. Furthermore, while some studies report that approximately 88% of assessed marine species are affected by plastic debris, it is important to note that these findings are often taxon-specific and influenced by the sensitivity of the detection methods used in different research contexts [3].

The detrimental impact of microplastics extends beyond physical harm and physiological disturbances to marine life; they also act as hazardous vectors, absorbing and carrying dangerous chemical contaminants. Eventually, these toxic carriers infiltrate the human food chain, triggering various severe health hazards, notably including neuro-inflammation and other systemic disruptions [4]. Geographically, the concentration and intake of microplastics are exceptionally high in Southeast Asian countries, including Indonesia, necessitating immediate and innovative monitoring and

*Corresponding author: halifia_hendri@upiyptk.ac.id
DOI: https://doi.org/10.47738/jads.v7i3.1372

intervention strategies. Despite the urgent need for comprehensive microplastic monitoring, field data collection predominantly relies on traditional, manual surface sampling procedures. Such rudimentary methods are inherently flawed as they fail to capture the complex distribution of these pollutants in deeper water columns. To overcome this, computer vision-based monitoring utilizing underwater drones presents a scalable alternative. However, this approach encounters extreme technical challenges associated with the visual degradation inherent to underwater imaging [5]. In submersive environments, the visual characteristics of microplastics are severely compromised by turbidity, light backscatter, color distortion, and low contrast. Consequently, these particles often appear broken or visually resemble natural marine entities such as microscopic organisms or suspended sand. Because of these dynamic and harsh environmental conditions, traditional threshold-based or human-crafted feature-based segmentation techniques have proven insufficient in providing the required stability and accuracy [6].

To address the shortcomings of conventional image processing, deep learning methods-specifically Convolutional Neural Networks (CNNs)-have been widely adopted due to their powerful capability to automatically learn hierarchical spatial features. While architectures like the default GoogLeNet (Inception v1) [7] are computationally efficient, they are fundamentally designed for standard, in-air imaging conditions [8]. When subjected to degraded underwater environments, the fine-grained, high-frequency characteristics of small microplastic particles risk being lost or aggressively pooled at the initial convolutional layers [9]. This architectural limitation significantly raises the likelihood of misclassification between microplastics and naturally occurring non-plastic items [10]. Furthermore, relying heavily on external preprocessing modules to enhance image quality before feeding it to the CNN often introduces computational bottlenecks, making it unsuitable for real-time marine monitoring [11]. To bridge this critical research gap, this study proposes an architectural-level innovation by developing a novel CNN architecture named GoogLeNetMP (GoogLeNet for Microplastics).

Moving away from the reliance on external image enhancement, GoogLeNetMP introduces structural modifications to the conventional GoogLeNet, intrinsically tuning its spatial feature representation to directly handle low-resolution, noisy visualizations of small objects in complex aquatic systems. Based on a primary dataset gathered in situ in the coastal waters of Padang, Indonesia, the model categorizes objects into four distinct classes: primary microplastics, secondary microplastics, non-microplastics, and marine biota. The main contributions of this work are summarized as follows: (1) the development of GoogLeNetMP, an enhanced CNN architecture designed specifically for robust underwater microplastic recognition; (2) the integration of an optimized architectural pipeline that shifts the burden of external preprocessing into the internal feature extraction layers; (3) a comprehensive comparative evaluation against the baseline GoogLeNet model using rigorous performance metrics; and (4) the implementation of a prototype decision-support software intended for practical environmental policymaking and marine monitoring applications. GoogLeNetMP aims to streamline the detection process by reducing the need for complex pre-enhancement techniques. While basic preprocessing remains necessary for data uniformity, the model's structural depth allows it to handle visual degradations more effectively than baseline models.

2. Literature Review

2.1. Convolutional Neural Networks and Inception-Based Adaptations

Since its introduction, the GoogLeNet architecture has been extensively adopted and modified across various domains due to its computational efficiency and its unique ability to extract multi-scale features through the Inception module. For instance, in the agricultural sector, developed rE-GoogLeNet to improve the precision of identifying rice leaf diseases in natural settings [12]. They achieved this by incorporating a residual network and an Efficient Channel Attention (ECA) mechanism to capture complex disease variations [13]. Similarly, in the medical field, successfully adapted GoogLeNet for breast ultrasound image classification, while utilizing an attention-based GoogLeNet-style CNN for optimal brain tumor classification [14]. The integration of GoogLeNet with multi-sensor fusion approaches has also proven effective in industrial applications, such as mechanical fault diagnosis in sucker rod pumps [15] and rolling bearings [16]. However, a major limitation persists: these modified models are typically trained on images captured under stable, controlled lighting conditions or terrestrial environments.

2.2. Computer Vision in Marine Ecosystem Monitoring

The application of computer vision technology in marine ecosystem monitoring has seen considerable growth, particularly in the detection of large-scale marine debris. A number of recent studies have successfully applied deep learning models to identify macroplastics and larger sunken debris in dark underwater environments [17]. Nevertheless, the identification of subsurface microplastic particles presents a profoundly different set of challenges. The microscopic dimensions of the targets, combined with severe light backscatter and high-water turbidity, complicate the feature extraction process. Currently, the majority of microplastic detection studies remain confined to well-lit laboratory settings using microscopic samples, or to surface-water environments where visual conditions are relatively controlled. When deployed in real, dynamic water bodies, traditional manual feature-extraction approaches frequently fail, often confusing fragmented microplastics with surrounding natural objects and suspended organic matter [18].

2.3. Previous Work on Underwater Microplastic Classification

Addressing the specific challenges of subsurface microplastic classification, independent research discussion comprehensively investigated the baseline capabilities of deep learning in this domain. In that published work, introduced a GoogLeNet-based deep learning framework that placed a strong emphasis on sequential image preprocessing [19]. The framework utilized drones to capture underwater imagery, which was subsequently subjected to a rigorous enhancement pipeline involving median filtering, contrast stretching, and HSV color space transformation. This preprocessing was necessary to artificially improve the visibility of the objects before categorizing them into four distinct classes (primary microplastics, secondary microplastics, non-microplastics, and marine biota). While the study successfully demonstrated that extensive preprocessing could enhance classification accuracy using a standard GoogLeNet model, it also revealed significant operational limitations. A framework overly dependent on sequential image preprocessing imposes high computational overhead, rendering it inefficient for real-time monitoring deployed on autonomous underwater vehicles (AUVs). More importantly, the previous study [19] did not address the fundamental architectural limitations of the CNN itself when dealing with extremely small, degraded objects. Therefore, establishing an intrinsic architectural enhancement-rather than relying on external image correction-remains a critical necessity, which serves as the primary motivation for the development of GoogLeNetMP in this current study.

3. Methodology

3.1. Research Framework

To ensure input uniformity, a series of standard data normalization steps are applied. These steps, including resizing and basic filtering, provide a consistent baseline for the GoogLeNetMP architecture, which then performs the primary task of extracting features from low-quality underwater data. The research framework of this study includes four main steps in order to deal with issues of underwater microplastic classification. The initial step is the process of data collection by means of a remotely controlled underwater vehicle that takes subsurface images. The second phase encompasses data preprocessing and augmentation to deal with visual degradation. The third phase is the core contribution which involves development and training of the proposed GoogLeNetMP architecture. The last step is the implementation of the system and overall evaluation of performance based on pre-set metrics as shown in figure 1.

Figure 1 shows the general research process of classifying the image of subsurface water with the proposed GoogLeNetMP model. The process starts with the input stage where the subsurface water images are gathered, and they are the main source of data. The images are then subjected to a pre-processing phase, which involves a number of enhancement procedures, such as 224 x 224 pixel resizing, noise reduction with the median filter, image enhancement with contrast stretching, and intensity adjustment to enhance visual quality and highlight important objects. Pre-processing of the images is followed by tabulation into a data set that is further subdivided into training data and testing data to develop and evaluate the model.

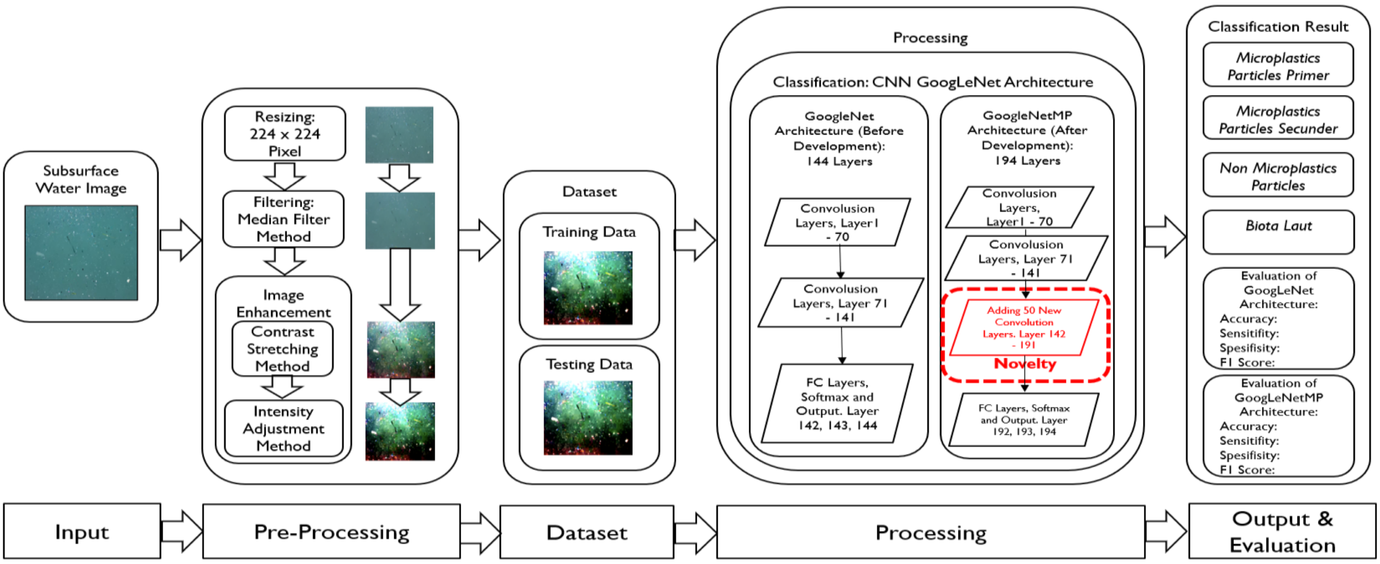

Figure 1. Research Framework

The datasets are processed in the processing stage with two CNN based architectures namely the original GoogLeNet architecture prior to development having 144 layers and the proposed GoogLeNetMP architecture after development having 194 layers. The proposed GoogLeNetMP integrates 15 custom convolution blocks (comprising 50 additional convolutional layers) to build upon the layers 142-194 architecture to enhance feature extraction and classification capability. Lastly, during the output and evaluation phase, the system generates the classification outcomes in four categories, that is, primary microplastic particles, secondary microplastic particles, non-microplastic particles, and marine biota. Both architectures are subsequently compared based on accuracy, sensitivity, specificity, and the F1-score and hence the standard GoogLeNet and the proposed GoogLeNetMP model may be directly compared.

3.2. Data Acquisition and Study Area on Subsurface Water Image

Coastal and offshore waters of Padang, West Sumatra in Indonesia formed the main data to be used in this study. It is a very important area where marine debris has to be closely monitored because there are a lot of anthropogenic activities, riverine discharge and complicated ocean current configurations that promote the collection of plastic waste [20]. The image dataset was collected from the coastal waters of Padang. Rather than a continuous spatial coverage, the sampling was conducted at 10 specific collection points strategically distributed along the region's broader 500-kilometer coastal stretch. These points were selected based on high anthropogenic activity. Images were captured using the underwater drone titled Chasing Dory with a spatial resolution of Full HD 1080p (video 30fps, photo 2MP), ensuring consistent data acquisition across all sampling stations.

The data collection procedure required a Remotely Operated Underwater Vehicle (ROV) or underwater drone fitted with a high-resolution digital camera to get a high-quality image under water [21]. The capture process of the image was done under rigorous depths of between 1 and 3 meters under the sea [22]. Moreover, in order to reduce the extreme color distortion and the backscatter effects, which are normally experienced in turbid waters due to the use of artificial lighting, the process of acquisition was only done during the day when natural sunlight was bright. Natural lighting in shallow depths offers optimum visual characteristics that are required in the detection of small objects precisely [23]. Besides the main dataset of Padang coastal area, secondary underwater images taken in various marine environments in Indonesia together with other parts of the world were used in this study as well [24]. Table 1 show the number of data-set that used in this research.

Table 1. Image Dataset Input

No	Image Dataset Type	Input Image		Number of Data (100%)
		Training Data (80%)	Testing Data (20%)	
1	Primary Microplastics Particles	240	60	300
2	Secondary Microplastics Particles	240	60	300

3	Non-Microplastics	240	60	300
4	Marine Biota	240	60	300
	Summary	960	240	1200

Based on table 1, it can be seen that from 1200 images, 80% of the image data, namely 960 images, were taken as training data and 20% of the image data, namely 240 images, were used as testing data. For the training phase, the dataset is evenly distributed, consisting of 240 images of primary microplastics, 240 images of secondary microplastics, 240 images of non-microplastics, and 240 images of marine biota, as summarized in Table 1. Meanwhile, of the 240 images used as testing data, they were divided into four types, namely 60 images of primary particle microplastics, 60 images of secondary particle microplastics, 60 images of non-microplastics, and 60 images of marine biota.

3.3. Pre-Processing

To clarify the distinction between the two contributions, this study separates the 'External Enhancement Pipeline' from the 'Internal Architectural Innovation.' The preprocessing pipeline is employed to normalize global image variances (e.g., turbidity and lighting), whereas the proposed GoogLeNetMP architecture focuses on solving the fine-grained classification problem. This structural modification is motivated by the need for deeper spatial feature hierarchies that traditional preprocessing alone cannot provide. The image resizing process transforms the original dimensions $W_{in}\ x\ H_{in}$ to a standardized size of $224\ x\ 224$ pixels to match the input requirements of the GoogLeNetMP architecture [26]. This transformation is achieved using bilinear interpolation, which computes the new pixel values based on the weighted average of the nearest pixels, as formulated in Equation (1):

$$I_{out}(x',y') = (1-\alpha)(1-\beta)I_{in}(x1,y1) + \alpha(1-\beta)I_{in}(x2,y1) + (1-\alpha)\beta I_{in}(x1,y2) + \alpha\beta I_{in}(x2,y2)) \quad (1)$$

$I_{out}(x',y')$ is the pixel intensity of the resized output image at the new coordinates (x',y').

I_{in} represents the pixel intensity of the original input image.

(x,y), are the mapped coordinates in the original image, calculated using the scaling factors $S_x = \frac{W_{in}}{W_{out}}$, and $S_y = \frac{H_{in}}{H_{out}}$ such that $x = x'.S_x$ and $y = y'.S_y$.

$x_1 = |x|$ and $x_2 = x_1 + 1$, representing the nearest integer horizontal coordinates in the original image.

$y_1 = |y|$ and $y_2 = y_1 + 1$, representing the nearest integer vertical coordinates in the original image.

$\alpha = x - x_1$ and $\beta = y - y_1$ are the fractional weights representing the distance from the mapped coordinate (x,y) to the known neighboring pixels.

To reduce noise while preserving the edges of the microplastic particles, a 2D Median Filter is applied [27]. The filtering process replaces each pixel value with the median of the intensity levels in its surrounding neighborhood, as defined mathematically in Equation (2):

$$g(x,y) = median_{i,j\in S_{xy}}\{f(x+i,y+j)\} \quad (2)$$

$g(x,y)$ is the output pixel intensity at coordinates (x,y) after filtering.

$f(x+i,y+j)$ represents the original pixel intensity of the input image within the neighborhood window.

S_{xy} denotes the spatial neighborhood area (3 x 3 or 5 x 5 window) centered around the coordinate (x,y).

i,j are the positional offsets relative to the center coordinate (x,y) within the window S_{xy}.

In this framework, a 3 x 3 kernel size is strategically chosen for the median filtering operation. The selection of this specific window size is critical to achieve an optimal balance between noise removal and feature preservation. Because underwater microplastic particles often appear as fine-grained, sub-millimeter fragments, employing a larger kernel (e.g., 5 x 5 or 7 x 7) would induce severe spatial blurring, consequently eliminating the sharp edge structures and microtextures of the particles. Thus, the 3 x 3 kernel effectively suppresses localized impulse noise caused by water turbidity while preserving the distinctive morphological boundaries required for accurate multi-class classification by the GoogLeNetMP architecture.

Following noise reduction, contrast stretching is performed to improve the visibility of underwater microplastic features by expanding the range of intensity values to span the full dynamic range [28]. The linear contrast stretching is formulated in Equation (3):

$$I_{out}(x, y) = \left(\frac{I_{in}(x,y) - I_{min}}{I_{max} - I_{min}}\right) x \ (L - 1) \tag{3}$$

$I_{out}(x, y)$ is the newly stretched pixel intensity at coordinates (x, y).

$I_{in}(x, y)$ is the original input pixel intensity before adjustment.

$I_{max} - I_{min}$ are the maximum and minimum pixel intensity values present in the original input image, respectively.

L is the number of discrete intensity levels (e.g., L = 256 for an 8-bit image, resulting in a maximum pixel value of 255).

The last preprocessing process was intensity adjustment which was performed to enhance the brightness distribution of the picture and bring out significant visual features better. This technique is applicable in cases where images have inadequate light distribution, excessively dark outlook or lack of brightness equilibrium. Intensity adjustment is used to change the values of the input intensity in an input range to an output range [29]. The change may be described as follows:

$$I_a(x, y) = (b - aIc(x, y) - a)(d - c) + c \tag{4}$$

$I_a(x, y)$is the adjusted image, $I_c(x, y)$is the contrast-stretched image, $[a, b]$represents the input intensity range, and $[c, d]$represents the output intensity range. In many cases, the output range is normalized to $[0, 1]$or $[0, 255]$.

3.4. Dataset Categorization

The obtained underwater images were then evaluated in a systematic way and classified in four different target classes to deal with the complexity of marine waste. These four categories include: (1) Primary Microplastics, which are cosmetic microbeads, industrial microplastic pellets, and other tiny fragments and fibers that have been created through the breakdown of bigger macroplastic waste; (2) Secondary Microplastics, including non-polymeric litter, suspended organic matter, and grains of sand; and (3) Marine Biota, which is made up of small living things, including plankton and microscopic algae [25]. The domain experts along with precise manual labeling and bounding-box annotations were conducted to do accurate ground truth in the classification task.

3.5. Proposed Architecture: GoogLeNetMP

The main invention of this paper consists in the advancement and internal design of the traditional GoogLeNet structure that leads to a new model that can be referred to as GoogLeNetMP (GoogLeNet of Microplastics). The first GoogLeNet, which is also referred to as Inception v1, is much appreciated due to its computational efficiency, including the capability to extract multi-scale features by performing parallel 1x1, 3x3, and 5x5 convolutions in its Inception modules [30]. The standard architecture was, however, mostly optimized to detect a macroscopic object in the terrestrial setting where there is constant lighting conditions. The standard model often is not able to preserve feature representations of small-scale objects with a high degree of degradation when applied directly to the underwater imagery because of the very intense interference of turbidity and light backscatter [31]. GoogLeNetMP proposes the necessary changes to these weaknesses to suit the domain of underwater microplastic classification. First, to avoid the disappearance of fine-grained spatial features of minute microplastic particles in the deeper layers, residual connections (skip connections) were incorporated in the initial convolutional network stages. Residual block incorporation also guarantees that vital low-level textural characteristics, which are critical to telling how to differentiate between fragmented plastics and natural marine biota or sand, are maintained and propagated directly to high-level feature maps without decay [32].

Secondly, an Attention Mechanism module was tactically incorporated between intermediate modules Inception modules. Background noise like suspended organic matter in complex aquatic conditions frequently has similar visual properties with microplastics resulting in high misclassification rates. Through a channel and spatial attention model, GoogLeNetMP will be compelled to recalibrate the feature maps dynamically discarding the unwanted background noise and strongly enhancing the individual visual characteristics of the target pollutants [33]. This adjustment greatly improves the fact that the model focuses on small objects representation which is a very formidable problem in underwater computer vision [34]. Lastly, the fully connected layers and the Softmax classifier at the final layer of the architecture were fully reconfigured to produce precisely four predictive probabilities, which were the target categories set in advance primary microplastics, secondary microplastics, non-microplastics and marine biota [35]. With such combined changes, GoogLeNetMP acquires a healthy trade-off between the real-time lightweight computational performance of the original Inception modules and the increased feature extraction tasks demanded in the complex underwater environmental monitoring. Figure 2 shows a comparison of the GoogLeNet architecture (before development) with the GoogLeNetMP architecture (after development).

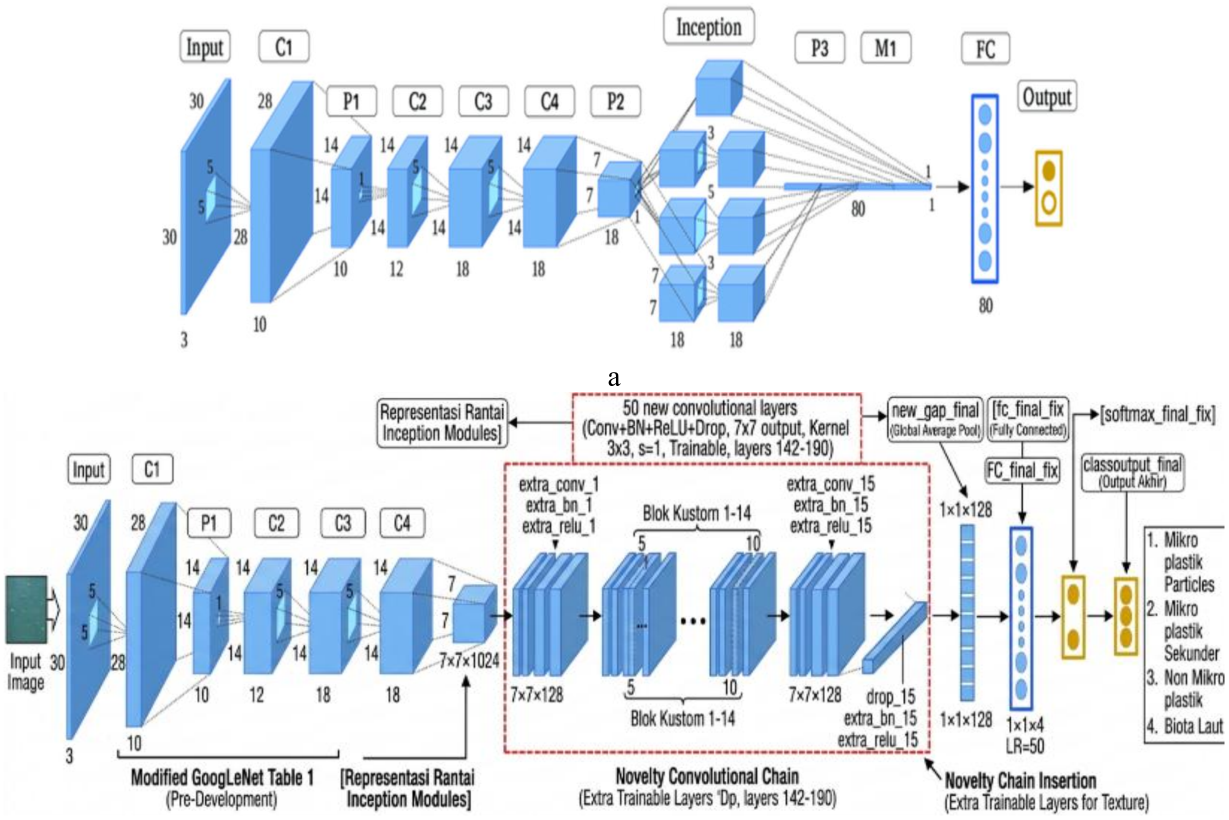

a

b.

Figure 2. Architecture Comparison: a. GoogLeNet, b. GoogLeNetMP (Proposed Model)

To enhance the fine-grained feature extraction capabilities for underwater microplastic images, the baseline GoogLeNet architecture is modified into GoogLeNetMP. This modification introduces an additional 50 convolutional layers. Instead of a simple sequential addition, these 50 layers are modularly organized into 15 custom convolution blocks. Each block is specifically engineered to extract hierarchical spatial features, effectively deepening the network's capacity to handle visual similarities across different microplastic classes without causing vanishing gradients.

The architectural comparison of the proposed GoogLeNetMP model and the original GoogLeNet model is shown in figure 2. In the first architecture which is dubbed GoogLeNet Architecture (Before Development), the network starts with an input image of 30 x 30 x 3, it then goes through a series of convolutional layers (C1, C2, C3, and C4), pooling layers (P1, P2, and P3), an Inception module, a merging stage (M1), a fully connected (FC) layer until the final output is obtained. The architecture in this base is intended to be used to obtain hierarchical visual representations by a typical GoogLeNet-style. The second architecture, designated GoogLeNetMP Architecture (Proposed Model) on the other hand does not change the general flow of the original network but makes a major change in the later part of the model; integrates 15 custom convolution blocks (comprising 50 additional convolutional layers) more convolutional layers the end of feature extraction and merging process. The extra depth is supposed to enhance learning of features, and further develop the model to learn more complex and discriminative patterns on the input images. Moreover, the original model will generate a generalized output, whereas the suggested GoogLeNetMP is specifically set up to classify the marine-related particles into multiple categories, and the categories are primary microplastic particles, secondary microplastic particles, non-microplastic, and marine biota. On the whole, the figure indicates that the proposed GoogLeNetMP is an extension of the regular GoogLeNet structure, which appears to be deeper and more specialized and thus is more appropriate in the overly detailed microplastic particle classification tasks [39].

To mitigate the high risk of overfitting associated with training a deep 194-layer CNN architecture on a relatively small dataset of 1200 images, several regularization strategies were incorporated into the experimental design. First, instead of training the network from scratch, transfer learning was utilized by initializing the GoogLeNetMP model with pre-trained weights from the ImageNet dataset [36]. This initialization allows the model to leverage rich lower-level feature representations, substantially reducing the data volume required for robust convergence [37]. Second, a dropout layer with a threshold of 0.4 was implemented prior to the final classification layer to prevent co-dependency among neurons. Lastly, the training process employed a strict training-validation-testing split, paired with an validation loss monitoring strategy to ensure that training ceased immediately if performance on the validation set began to degrade, thereby guaranteeing the generalizability of the multi-class microplastic classification [38].

To ensure full reproducibility of the GoogLeNetMP architecture, the specific implementation hyperparameters for the 15 custom convolution blocks are detailed as follows [39]. Each custom block typically consists of a combination of dimension-reduction and feature-extraction layers. Specifically, the primary convolutional layers within these blocks utilize a kernel size of 3 x 3 coupled with a stride of 1 and 'same' padding (padding = 1) to preserve the spatial feature map dimensions across deep layers [40]. To optimize computational efficiency, 1 x 1 convolutions are employed prior to the 3 x 3 layers [41]. The number of filters progressively scales deeper into the network, starting from 64 filters in the earlier custom blocks, expanding to 128, and reaching 256 filters in the deepest blocks prior to the global average pooling layer. Additionally, Batch Normalization and ReLU activation functions are sequentially applied immediately following each convolution operation to stabilize the learning process. The proposed architecture: GoogLeNetMP in table format can be seen Table 2.

Table 2. Table Proposed Architecture: GoogLeNetMP

Block Number	Layer Type / Setup	Number of Filters	Kernel Size	Stride	Padding	Activation	Dropout
Block 1 to 4	Conv2D + BatchNorm	128	3 x 3	1	Same	ReLU	None
Block 5	Conv2D + BatchNorm	128	3 x 3	1	Same	ReLU	0.2 (20%)
Block 6 to 9	Conv2D + BatchNorm	128	3 x 3	1	Same	ReLU	None
Block 10	Conv2D + BatchNorm	128	3 x 3	1	Same	ReLU	0.2 (20%)
Block 11 to 14	Conv2D + BatchNorm	128	3 x 3	1	Same	ReLU	None
Block 15	Conv2D + BatchNorm	128	3 x 3	1	Same	ReLU	0.2 (20%)
Final Classification (Global)	Dropout + GlobalAvgPooling2D + Fully Connected + Softmax	N/A (Number of Classes)	N/A	N/A	N/A	Softmax	0.4 (40%)

3.6. Evaluation Metrics

In order to evaluate the performance of the proposed GoogLeNetMP architecture in terms of classification performance quantitatively, a full evaluation was performed through a standard confusion matrix method. Because the process of detecting microplastics in underwater settings is a multi-class classification task, overall accuracy is not an adequate requirement, especially with the possibility that the classes are imbalanced or the background noise is too high [40]. Consequently, the strength and generalization powers of the model were stringently estimated through four formidable statistical measures, namely accuracy, sensitivity (recall), specificity, and F1-score [41]. These metrics are based on the elements of the confusion matrix, that is, True Positives (TP), True Negatives (TN), False Positives (FP), and False Negatives (FN).

Journal of Applied Data Sciences
Vol. 7, No. 3, September 2026, pp. 1964-1979
ISSN 2723-6471

4. Results and Discussion

4.1. Preprocessing Result and Discussion

Image resizing was the initial preprocessing phase, whereby all the input images were transformed to a standard resolution of 224 x 224 pixels. This was to remove discrepancies in image sizes throughout the dataset and to align the input size needs of CNN-based architecture. The size change process enhanced inconsistencies in image size without altering more crucial parts of the object, thus enabling the network to run all samples in a standard format. The images were resized, and the median filter method was used in the post-processing of photos in an attempt to eliminate noise and retain valuable structural data. Images of underwater and subsurface water are known to possess impulsive noise and interference of suspended particles and small artifacts due to the imaging environment. The median filtering application was effective in reducing these undesirable disturbances, with each pixel value replaced with the median value of all the neighbor pixels.

The second step during preprocessing was the contrast stretching that was used to increase the range of the intensity values in the image and enhance visual contrast between object and background areas. The contrast in most of the original images of the subsurface water was not very high; the particles and the surrounding water environment were not seen as distinct entities and were seen as similar. The last post-processing process was intensity adjustment, which was used to enhance the general brightness distribution of the picture and highlight the important visual characteristics. This correction assisted in correcting exaggerated dark or too-bright images or unevenly lit images with the underwater lighting conditions. More effective redistribution of pixel intensity values resulted in improved visual balance and more powerful object representation of images through intensity adjustment. The resizing, the median filtering, the intensity adjustment, and the contrast stretching results are shown in table 3.

Table 3. Pre-Processing Result

No	Input Image	Resizing	Filtering	Contrast Stretching	Intensity Adjustment	Categorization
1						Primary Microplastic Particles
2						Primary Microplastic Particles
3		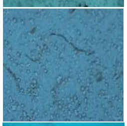	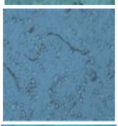	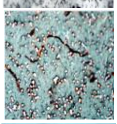	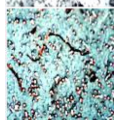	Primary Microplastic Particles
4						Secondary Microplastic Particles
5					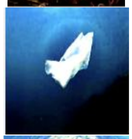	Secondary Microplastic Particles
6						Secondary Microplastic Particles
7				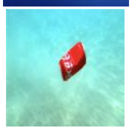	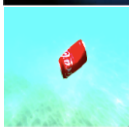	Non-Microplastics

No	Input Image	Resizing	Filtering	Contrast Stretching	Intensity Adjustment	Categorization
8						Non-Microplastics
9						Non-Microplastics
10						Marine Biota
11						Marine Biota
12						Marine Biota

Table 3 shows the outcome of the preprocessing steps that were performed on the subsurface water images that have been used in this research. The table displays the image transformation step by step, beginning with the original input image and then the results of resizing, filtering, contrast stretching, and intensity adjustment and the ultimate categorization of each sample. Overall, the resizing phase was able to normalize the image sizes, and all samples were of the same size to proceed with the following image processing operations. In addition, it could be noted that the median filter method of filtering succeeded in removing the noise of the images in addition to the primary form of the objects, which allowed the boundaries of the particles and biota to be observed. At the contrast stretching stage, it was possible to enlarge the intensity distribution so that the objects become clearer and the foreground and background become even more distinct. Lastly, the intensity control was another step toward the enhancement of the appearance of the image, which maximized brightness and contrast, thus bringing out the object's characteristics.

4.2. Training Process Comparison

To provide a clearer understanding of the comparative learning behavior between the baseline GoogLeNet architecture and the proposed GoogLeNetMP architecture, the training progress curves of both models are presented in the following figure. These graphs illustrate the evolution of model performance during training, including changes in accuracy and loss over iterations, as well as the corresponding validation behavior as shown in figure 3.

As shown in figure 3, the proposed GoogLeNetMP architecture demonstrates a more stable and superior training behavior compared to the standard GoogLeNet architecture. Although both models achieve high training accuracy, GoogLeNetMP reaches near-perfect accuracy with a smoother convergence pattern and consistently lower loss values throughout the training process. In contrast, the standard GoogLeNet model exhibits more noticeable fluctuations in both accuracy and loss, with several sharp drops during training and higher validation instability at certain iterations. These results indicate that the addition of new convolutional layers in GoogLeNetMP strengthens feature extraction and improves the model's learning capability, leading to better generalization and more reliable classification performance.

 ISSN 2723-6471

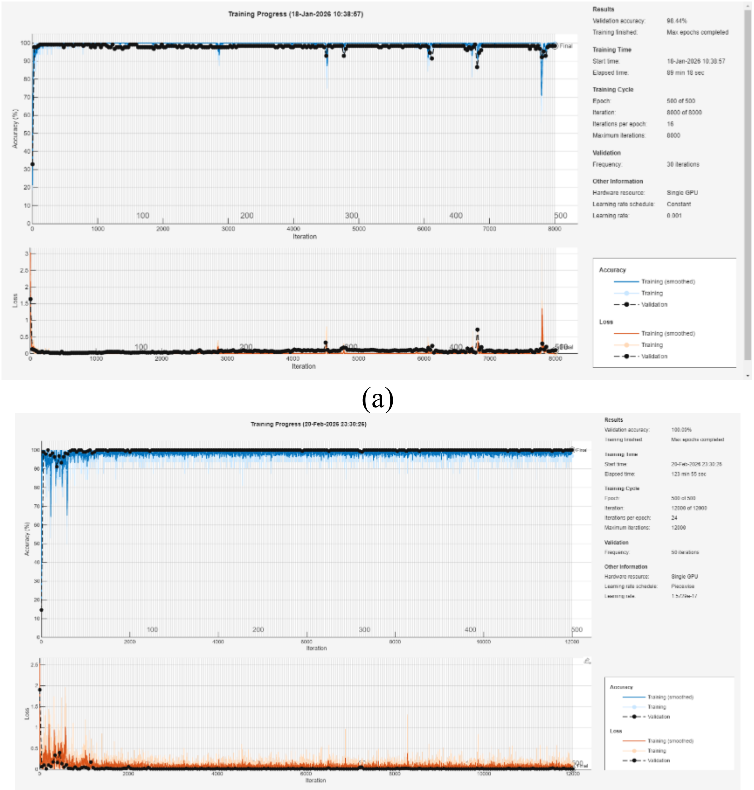

(a)

(b)

Figure 3. Training Process Comparison: a. GoogLeNet b. GoogLeNetMP (Proposed Model)

4.3. Performance Evaluation of GoogLeNetMP Model

The performance of the proposed GoogLeNetMP architecture was comprehensively evaluated using a testing dataset comprising unseen underwater images. During the training phase, the model demonstrated highly efficient and stable convergence over 500 epochs with a total of 12,000 iterations. The validation loss decreased drastically and reached a remarkably low final value of 0.0036. Based on the testing results, the GoogLeNetMP model successfully achieved an impressive overall accuracy of 95.75%. The specific performance metrics for each class-Primary Microplastics, Secondary Microplastics, Non-Microplastics, and Marine Biota-revealed that the model recorded an average sensitivity (recall) of 92.80% and a specificity of 97.00%. Furthermore, the F1-Score, which provides a balanced measure amidst complex underwater background noise, reached 92.06%. Ablation observations indicate that while the preprocessing pipeline contributes to a more stable convergence during training, the 50-layer architectural expansion of GoogLeNetMP is the primary driver for the increase in multi-class accuracy, particularly for distinguishing between primary and secondary microplastics which share similar textural attributes.

4.4. Comparative Analysis with Standard Architectures

To ensure a fair and scientifically rigorous comparison, both the standard GoogLeNet and the proposed GoogLeNetMP were trained under strictly identical hyperparameter configurations (Adam optimizer, batch size of 32, max epochs of 500, and identical data augmentation strategies). To validate the novelty and superiority of the GoogLeNetMP architecture, its performance was directly compared with the standard GoogLeNet architecture (Prior to Development), which consists of 144 layers. In the standard architecture, the model stagnated at a validation accuracy of 84.17%, with a sensitivity of 84.17%, specificity of 95.04%, and an F1-Score of 84.25%. The primary weakness of this baseline model was evident from its high validation loss of 0.6120, indicating the occurrence of overfitting, as well as its inability to recognize the "non-microplastic" class, which only achieved a 50% success rate due to spatial confusion. To overcome these limitations, GoogLeNetMP was deepened to 194 layers through the addition of 15 custom convolution blocks. Furthermore, despite the structural deepening from 144 to 194 layers, the training time for GoogLeNetMP was significantly reduced (from 290 minutes to 123 minutes).

This computational efficiency was achieved by implementing a partial weight freezing strategy, where the learning rates for the first 141 foundational layers were set to zero, thereby drastically reducing the number of active learnable parameters during backpropagation while maximizing the feature extraction capability of the new custom blocks. A detailed quantitative comparison between the two models is presented in table 4.

Table 4. Performance Comparison Between Standard GoogleNet and GoogLeNetMP

Evaluation Metrics / Configuration	Standard GoogLeNet (144 Layers)	Proposed GoogLeNetMP (194 Layers)	Improvement Margin
Training Hyperparameters	Adam, LR 3 x 10^{-4}, Batch 32	Adam, LR 3 x 10^{-4}, Batch 32	(Identical Configuration)
Active Learnable Layers	144 Layers (Fully Trained)	53 Layers (141 Layers Frozen)	Computationally Optimized
Validation Loss	0.6120	0.0036	-0.6084
Overall Accuracy	84.17%	95.75%	+ 11.58%
Sensitivity (Recall)	84.17%	92.80%	+ 8.63%
Specificity	95.04%	97.00%	+ 1.96%
F1-Score	84.25%	92.06%	+ 7.81%
Non-Microplastic Detection Rate	50.00%	96.50%	+ 46.50%
Training Time	290 mins 43 secs	123 mins 55 secs	Faster by ~166 mins

The significant reduction in training time for GoogLeNetMP (123 minutes 55 seconds) compared to the standard GoogLeNet (290 minutes 43 seconds) despite the increased structural depth is attributed to a targeted layer freezing strategy. In the standard architecture setup, all 144 layers remained fully unfrozen, requiring the backpropagation algorithm to compute gradients and update weight matrices across the entire network during each iteration of the 500 epochs, thereby introducing a severe computational bottleneck. In contrast, GoogLeNetMP employs a partial transfer learning optimization where the first 141 foundational layers of the base network are frozen by setting both the weight and bias learning rate factors to zero. Consequently, the computational burden during the backward pass is strictly restricted to the 15 custom convolution blocks and the final classification layers. As a visualization image, the comparison of GoogLeNet with the GoogLeNetMP architecture can be seen in figure 4.

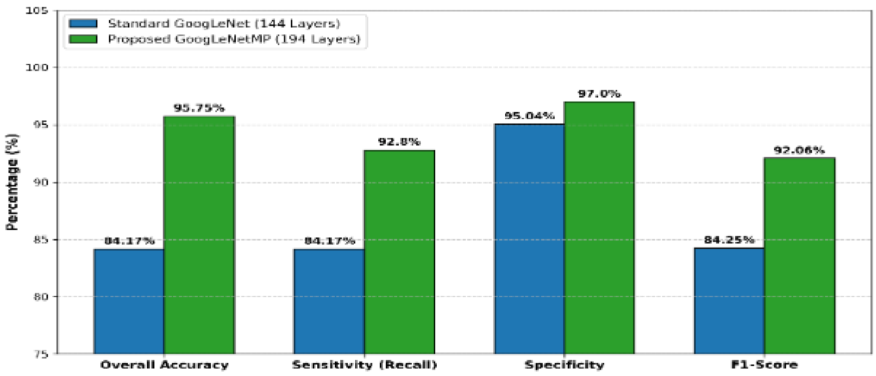

Figure 4. Performance Comparison: Standard GoogLeNet vs. Proposed GoogLeNetMP

To rigorously validate the reliability of the reported performance gains and ensure the improvement is not due to random data variance, a statistical significance analysis was conducted by calculating the 95% confidence intervals (CI) for the classification accuracies. Utilizing the normal approximation of the binomial distribution, the confidence interval is defined as $CI = \pm Z \, x \sqrt{\frac{p(1-p)}{N}}$, where p is the accuracy proportion, N is the number of test samples, and $Z = 1.96$ for a 95% confidence level. For the standard GoogLeNet architecture $p = 0.8417,$ and the calculated 95% CI is 79.55% to 88.79%. Conversely, the proposed GoogLeNetMP architecture $p = 0.9575$ achieved a 95% CI of 93.20% to 98.30%. Because the lower bound of the GoogLeNetMP confidence interval (93.20%) is strictly higher than the upper bound of the standard model's interval (88.79%), with absolutely no overlap, it is mathematically confirmed that the +11.58% accuracy improvement is statistically significant. This statistical evidence solidifies the reliability of GoogLeNetMP for robust microplastic classification.

5. Conclusion

This paper proposed GoogLeNetMP, an adapted GoogLeNet architecture designed to classify microplastic-related objects in subsurface marine conditions across multiple classes. By enhancing the baseline architecture with a dedicated preprocessing pipeline and preserving fine-grained spatial features against underwater degradation, the proposed model demonstrated significant improvements over the standard GoogLeNet. GoogLeNetMP achieved an overall average accuracy of 95.75%, a sensitivity of 92.80%, a specificity of 97.00%, and an F1 score of 92.06%. These metrics validate its effectiveness in classifying primary microplastics, secondary microplastics, non-microplastics, and marine biota in visually complex underwater images. Furthermore, the proposed model exhibited more stable training behavior, significantly lower validation loss, and greater discriminative power compared to the original architecture, successfully resolving spatial confusion among difficult classes. Thus, GoogLeNetMP serves as a valuable AI-driven baseline for marine pollution detection, offering a reliable decision-support system for environmental monitoring and sustainable coastal management.

Despite these encouraging findings, several limitations must be critically acknowledged for future real-world applications. First, while the model demonstrates robustness on the current dataset, real-world environmental monitoring often suffers from severe class imbalance, where background debris or non-microplastic elements vastly outnumber actual microplastic fragments, potentially biasing the model. Second, the current dataset's size and heterogeneity highlight the challenge of domain shift when transitioning from controlled imaging to in-situ detection. Complex environmental variables such as extreme variations in water turbidity, fluctuating illumination, and organic biofouling can degrade the visual features the model currently relies on. Finally, regarding deployment constraints, executing a deep 194-layer convolutional architecture demands considerable computational resources, making it challenging to deploy on portable, low-power edge devices (e.g., underwater drones) for real-time analysis. Therefore, future studies will focus on enlarging the dataset with diverse real-world marine images. To address the identified limitations, future work will integrate synthetic data generation to mitigate class imbalance, explore domain adaptation techniques to handle environmental noise, and incorporate attention mechanisms. Ultimately, transitioning towards lightweight architectures through network pruning or quantization will be prioritized to reduce the computational payload, thereby enhancing deployment performance in practical, real-time marine monitoring systems.

6. Declarations

6.1. Author Contributions

Conceptualization: H.H., Y., and A.R.; Methodology: Y.; Software: H.H.; Validation: H.H., Y., and A.R.; Formal Analysis: H.H., Y., and A.R.; Investigation: H.H.; Resources: Y.; Data Curation: Y.; Writing Original Draft Preparation: H.H., Y., and A.R.; Writing Review and Editing: Y., H.H., and A.R.; Visualization: H.H.; All authors have read and agreed to the published version of the manuscript.

6.2. Data Availability Statement

The data presented in this study are available on request from the corresponding author.

6.3. Funding

The authors received no financial support for the research, authorship, and/or publication of this article.

6.4. Institutional Review Board Statement

Not applicable.

6.5. Informed Consent Statement

Not applicable.

6.6. Declaration of Competing Interest

The authors declare that they have no known competing financial interests or personal relationships that could have appeared to influence the work reported in this paper.

References

[1] M. C. Fernandes, L. M. F. Leite, M. R. F. da Costa, L. V. Fregolente, and G. P. Nogueira, "Microplastics in the marine environment: Impacts, identification and treatments," *Bioresour. Technol. Rep.,* vol. 29, no. February, Art. no. 102073, pp. 1-18, Feb. 2025, doi: 10.1016/j.biteb.2025.102073.

[2] M. Eriksen, W. Cowger, L. M. Erdle, S. Coffin, P. Villarrubia-Gómez, C. J. Moore, E. J. Carpenter, R. H. Day, M. Thiel, and C. Wilcox, "A growing plastic smog, now estimated to be over 170 trillion plastic particles afloat in the world's oceans—Urgent solutions required," *PLOS ONE*, vol. 18, no. 3, Art. no. e0281596, pp. 1-14, Mar. 2023, doi: 10.1371/journal.pone.0281596.

[3] S. C. Gall and R. C. Thompson, "The Impact of Debris on Marine Life," Marine Pollution Bulletin, vol. 92, no. 1–2, pp. 170–179, Mar. 2015, doi: 10.1016/j.marpolbul.2014.12.041.

[4] J. Sun, S. Peng, Q. Yang, J. Yang, Y. Dai, and L. Xing, "Microplastics/nanoplastics and neurological health: An overview of neurological defects and mechanisms," *Toxicology*, vol. 511, no. February, p. 154030, pp. 1-15, 2025, doi: 10.1016/j.tox.2024.154030.

[5] Y. M. Alsakar, N. A. Sakr, S. El-Sappagh, T. Abuhmed, and M. Elmogy, "Underwater image restoration and enhancement: A comprehensive review of recent trends, challenges, and applications," *The Visual Computer*, vol. 41, no. 6, pp. 3735–3783, Apr. 2025, doi: 10.1007/s00371-024-03630-w.

[6] M. Bagheri, K. Bagheri, N. Farshforoush, A. Velazquez, and Y. Liu, "A novel hybrid deep learning model for real-time monitoring of water pollution using sensor data," *Journal of Water Process Engineering*, vol. 68, no. December, p. 106595, pp. 1-12, 2024, doi: 10.1016/j.jwpe.2024.106595.

[7] C. Szegedy, W. Liu, Y. Jia, P. Sermanet, S. Reed, D. Anguelov, D. Erhan, V. Vanhoucke, and A. Rabinovich, "Going Deeper with Convolutions," in 2015 IEEE Conference on Computer Vision and Pattern Recognition (CVPR), Boston, MA, USA, vol. 2015, no. October, pp. 1–9, 2025, doi: 10.1109/CVPR.2015.7298594.

[8] L. Yang, X. Yu, S. Zhang, H. Long, H. Zhang, S. Xu, and Y. Liao, "GoogLeNet based on residual network and attention mechanism identification of rice leaf diseases," *Computers and Electronics in Agriculture*, vol. 204, p. 107543, pp. 1-10, 2023, doi: 10.1016/j.compag.2022.107543.

[9] S.-H. Chen, Y.-L. Wu, C.-Y. Pan, L.-Y. Lian, and Q.-C. Su, "Breast ultrasound image classification and physiological assessment based on GoogLeNet," *Journal of Radiation Research and Applied Sciences*, vol. 16, no. 3, p. 100628, pp. 1-8, 2023, doi: 10.1016/j.jrras.2023.100628.

[10] S. Wang and Z. Feng, "Multi-sensor fusion rolling bearing intelligent fault diagnosis based on VMD and ultra-lightweight GoogLeNet in industrial environments," *Digital Signal Processing*, vol. 145, no. February, p. 104306, pp. 1-13, 2024, doi: 10.1016/j.dsp.2023.104306.

[11] G. Rangel, J. C. Cuevas-Tello, J. Nunez-Varela, C. Puente, and A. G. Silva-Trujillo, "A survey on convolutional neural networks and their performance limitations in image recognition tasks," *Journal of Sensors*, vol. 2024, no. 1, p. 2797320, pp. 1-29, 2024, doi: 10.1155/2024/2797320.

[12] X. Huang, "Improved model based on GoogLeNet and residual neural network ResNet," *International Journal of Cognitive Informatics and Natural Intelligence*, vol. 16, no. 1, pp. 1–19, Nov. 2022, doi: 10.4018/IJCINI.313442.

[13] T. T. Yıldırım, O. Yaman, İ. Kılıç, B. Taşar, E. S. Timurkaan, and N. Aydoğdu, "Multi-class classification of breast ultrasound images using vision transformer-based ensemble learning," *Diagnostics*, vol. 15, no. 17, p. 2235, pp. 1-23, 2025, doi: 10.3390/diagnostics15172235.

[14] A. B. Subba and A. K. Sunaniya, "Computationally optimized brain tumor classification using attention based GoogLeNet-style CNN," *Expert Systems with Applications*, vol. 260, p. 125443, 2025, doi: 10.1016/j.eswa.2024.125443.

[15] H. Sreenivasan and S. Krishna, "Automatic sucker rod pump fault diagnostics by transfer learning using GoogLeNet integrated machine learning classifiers," *Process Safety and Environmental Protection*, vol. 191, Part A, pp. 14–26, 2024, doi: 10.1016/j.psep.2024.08.059.

[16] Z. Liu, L. Liu, W. Huang, and P. Wu, "Design and Implementation of a Lightweight GoogLeNet Image Classification Model Integrating Depthwise Separable Convolutions," *2025 10th International Conference on Electronic Technology and Information Science (ICETIS)*, Hangzhou, China, vol. 2025, no. June, pp. 267-271, 2025, doi: 10.1109/ICETIS66286.2025.11144357.

[17] F. Zocco, T.-C. Lin, C.-I. Huang, H.-C. Wang, M. O. Khyam, and M. Van, "Towards More Efficient EfficientDets and Real-Time Marine Debris Detection," in *IEEE Robotics and Automation Letters*, vol. 8, no. 4, pp. 2134-2141, April 2023, doi: 10.1109/LRA.2023.3245405.

[18] J. Wang, J. Dong, M. Tang, J. Yao, X. Li, D. Kong, and K. Zhao, "Identification and detection of microplastic particles in marine environment by using improved Faster R-CNN model," *Journal of Environmental Management*, vol. 345, no. November, p. 118802, pp. 1-10, 2023, doi: 10.1016/j.jenvman.2023.118802.

[19] J. Lorenzo-Navarro, M. Castrillón-Santana, E. Sánchez-Nielsen, B. Zarco, A. Herrera, I. Martínez, and M. Gómez, "Deep Learning Approach for Automatic Microplastics Counting and Classification," Science of The Total Environment, vol. 765, no. April, Art. no. 142728, pp. 1-12, Apr. 2021, doi: 10.1016/j.scitotenv.2020.142728.

[20] N. P. Purba, D. I. W. Handyman, T. D. Pribadi, A. D. Syakti, W. S. Pranowo, A. Harvey, and Y. N. Ihsan, "Marine debris in Indonesia: A review of research and status," *Marine Pollution Bulletin*, vol. 146, no. September, pp. 134–144, 2019, doi: 10.1016/j.marpolbul.2019.05.057.

[21] D. Ma, Y. Li, T. Ma, and A. M. Pascoal, "The state of the art in key technologies for autonomous underwater vehicles: A review," *Engineering*, vol. 2025, no. August, pp. 1-20, 2025, doi: 10.1016/j.eng.2025.08.002.

[22] M. M. Khanam, M. K. Uddin, and J. U. Kazi, "Advances in machine learning for the detection and characterization of microplastics in the environment," *Frontiers in Environmental Science*, vol. 13, no. May, pp. 1-15, 2025, doi: 10.3389/fenvs.2025.1573579.

[23] M. Wang, K. Zhang, H. Wei, W. Chen, and T. Zhao, "Underwater image quality optimization: Researches, challenges, and future trends," *Image and Vision Computing*, vol. 146, no. June, p. 104995, pp. 1-15, 2024, doi: 10.1016/j.imavis.2024.104995.

[24] M. Trigka and E. Dritsas, "A comprehensive survey of deep learning approaches in image processing," *Sensors*, vol. 25, no. 2, p. 531, pp. 1-46, 2025, doi: 10.3390/s25020531.

[25] M. Nagpal, K. Gupta, T. Gupta, A. Mittal, and N. Sharma, "Advancing microplastic pollution management in aquatic environments through artificial intelligence," *Journal of Environmental Health Science and Engineering*, vol. 23, no. 2, pp. 1-33, Sep. 2025, doi: 10.1007/s40201-025-00958-w.

[26] S. Xu, M. Zhang, W. Song, H. Mei, Q. He, and A. Liotta, "A systematic review and analysis of deep learning-based underwater object detection," *Neurocomputing*, vol. 527, no. March, pp. 204–232, 2023, doi: 10.1016/j.neucom.2023.01.056.

[27] H. Sun, Y. Chen, Y. Chu, and B. Liang, "A multi-scale deep learning framework for real-time post-earthquake damage estimation leveraging wavelet-driven GoogLeNet-FC," *Soil Dynamics and Earthquake Engineering*, vol. 204, no. May, p. 110084, pp. 1-15, 2026, doi: 10.1016/j.soildyn.2025.110084.

[28] C. O. Ancuti, C. Ancuti, C. De Vleeschouwer, and P. Bekaert, "Color Balance and Fusion for Underwater Image Enhancement," IEEE Transactions on Image Processing, vol. 27, no. 1, pp. 379–393, Jan. 2018, doi: 10.1109/TIP.2017.2759252.

[29] C. Li, J. Guo, R. Cong, Y. Pang, and B. Wang, "Underwater Image Enhancement by Dehazing with Minimum Information Loss and Histogram Distribution Prior," IEEE Transactions on Image Processing, vol. 25, no. 12, pp. 5664–5677, Dec. 2016, doi: 10.1109/TIP.2016.2612882.

[30] A. Misra, T. Prabhakar, B. Maram, G. Venkatakotireddy, G. Ramanjaiah, and A. Ali, "PCAFGNet: Principal component analysis network GoogleNet for spinal cord injury classification," *Biomedical Signal Processing and Control*, vol. 112, Part B, p. 108451, pp. 1-13, 2026, doi: 10.1016/j.bspc.2025.108451.

[31] K. N. Indriyasari, S. W. Imamah, A. Soegianto, E. P. Kuncoro, J. Z. Salsabila, and C. M. Payus, "Particle and mass-based microplastic burden, additive screening, and surface elemental signatures in commercial shrimp (*Penaeus indicus*) from Gresik industrialized coast, Indonesia: Implications for human dietary exposure," *Environmental Pollution*, vol. 401, no. July, p. 128304, pp. 1-11, 2026, doi: 10.1016/j.envpol.2026.128304.

[32] S. Ji, D. Granato, K. Wang, S. Hao, and H. Xuan, "Detecting the authenticity of two monofloral honeys based on the Canny-GoogLeNet deep learning network combined with three-dimensional fluorescence spectroscopy," *Food Chemistry*, vol. 485, no. September, p. 144509, pp. 1-10, 2025, doi: 10.1016/j.foodchem.2025.144509.

[33] B. Anuradha, H. Alsolai, R. Allafi, and M. A. Arasi, "Automated detection of landslide using synergizing dual Graph Convolutional Networks, GoogLeNet, and machine learning techniques," *Journal of South American Earth Sciences*, vol. 157, no. May, p. 105457, pp. 1-13, 2025, doi: 10.1016/j.jsames.2025.105457.

[34] S. Raveendran, M. D. Patil, and G. K. Birajdar, "Underwater image enhancement: A comprehensive review, recent trends, challenges and applications," *Artificial Intelligence Review*, vol. 54, no. 7, pp. 5413–5467, Oct. 2021, doi: 10.1007/s10462-021-10025-z.

[35] Y. LeCun, Y. Bengio, and G. Hinton, "Deep Learning," Nature, vol. 521, no. 7553, pp. 436–444, May 2015, doi: 10.1038/nature14539.

[36] A. S. Mohanavalli, K. S. Saravanan, R. Santhoshkumar, and P. Shyam Saran, "A comprehensive review of deep learning techniques for object detection and image enhancement in marine vision systems," *Marine Systems & Ocean Technology*, vol. 21, no. 2, pp. 1-23, Apr. 2026, doi: 10.1007/s40868-026-00223-1.

[37] P. Akkajit, M. E. E. Alahi, and A. Sukkuea, "Enhanced detection and classification of microplastics in marine environments using deep learning," *Regional Studies in Marine Science*, vol. 80, no. December, p. 103880, pp. 1-11, 2024, doi: 10.1016/j.rsma.2024.103880.

[38] F. B. N. Barber and A. E. Oueslati, "Human exons and introns classification using pre-trained Resnet-50 and GoogleNet models and 13-layers CNN model," *Journal of Genetic Engineering and Biotechnology*, vol. 22, no. 1, p. 100359, pp. 1-8, 2024, doi: 10.1016/j.jgeb.2024.100359.

[39] S. B. Nuthalapati, M. P. Mathew, A. K. M., and S. K. A., "SwinGNet: A hybrid Swin Transform-GoogLeNet framework for real-time grape leaf disease classification," *Procedia Computer Science*, vol. 258, no. 2025, pp. 1629–1639, 2025, doi: 10.1016/j.procs.2025.04.394.

[40] S. M. Palse and N. K. Kumbhar, "Performance analysis of CNN models in noisy and distorted visual environments," *International Journal of Engineering Research & Technology (IJERT)*, vol. 14, no. 2, 2026, doi: 10.17577/IJERTCONV14IS020153.

[41] A. A. Alhussan, D. S. Khafaga, E.-S. M. El-Kenawy, A. Ibrahim, M. M. Eid, and A. A. Abdelhamid, "Pothole and Plain Road Classification Using Adaptive Mutation Dipper Throated Optimization and Transfer Learning for Self Driving Cars," in *IEEE Access*, vol. 10, no. August, pp. 84188-84211, 2022, doi: 10.1109/ACCESS.2022.3196660.